

IMAGE RECONSTRUCTION IN POLYCHROMATIC INTERFEROMETRY

F. Soulez¹

Abstract. As the first VLT 4 telescopes beam combiner, PIONIER made routine interferometric imaging possible at the VLT. With its higher spectral resolution, GRAVITY will be able to produce hyperspectral images with the resolution of the millisecond of arc. However only few algorithms have been proposed for the reconstruction of such hyperspectral images. Among the various approaches for polychromatic reconstruction we present the MiRA-3D algorithm developed in Lyon and its results on simulations and data on PIONIER.

Keywords: Image reconstruction ; Optical interferometry ; VLT

1 Introduction

The objective of stellar interferometric imaging is to recover an approximation of the specific brightness distribution $I(\lambda, \boldsymbol{\theta})$ of the observed astronomical object given measurements which are sparse samples of the spatial Fourier transform $\hat{I}(\lambda, \boldsymbol{\nu})$ of $I(\lambda, \boldsymbol{\theta})$. In its simplest form, it consists on a coherent recombination of the light from a pair of telescopes pointing the same target. By varying the optical path delay between the two arms of the interferometer, one observes fringes. Without atmospheric turbulence, the contrast and the phase of those fringes are the amplitude ρ and the phase ϕ respectively of the complex value $\hat{I}(\lambda, \boldsymbol{\nu}) = \rho(\lambda, \boldsymbol{\nu}) \exp(\phi(\lambda, \boldsymbol{\nu}))$ at the spatial frequency $\boldsymbol{\nu} = B/\lambda$ with B the projected baseline between both telescopes.

Unfortunately all ground based interferometers are subject to atmospheric turbulence. This have mainly two consequences:

- the boiling of speckle patterns in the telescope focal plane causes random variation of the transmission $A_i(\nu, t)$ of each telescope i and thus the observed contrast of the fringes,
- it introduces a random delay in the optical path causing random variations of the observed phase.

The first problem is overcome by normalizing the observed contrast by the flux in the photometric channel of each telescope. As consequence, the estimated amplitudes are only relative to the integrated flux (*i.e.* the amplitude at $\boldsymbol{\nu} = 0$).

Two solutions are usually proposed to have an estimate of phases. The first is to measure the atmospheric random delay using a reference source. This phase reference is implemented in the GRAVITY beam combiner. The second solution is to measure quantities unaffected by such random delay, namely:

- powerspectrum: $P(\lambda, \boldsymbol{\nu}) = |\hat{I}(\lambda, \boldsymbol{\nu})|^2$,
- bispectrum: $B(\lambda, \boldsymbol{\nu}, \boldsymbol{\nu}') = \hat{I}(\lambda, \boldsymbol{\nu}) \hat{I}(\lambda, \boldsymbol{\nu}') \hat{I}^*(\lambda, \boldsymbol{\nu} + \boldsymbol{\nu}')$,
- phase closure: $\Psi(\lambda, \boldsymbol{\nu}, \boldsymbol{\nu}') = \arg B(\lambda, \boldsymbol{\nu}, \boldsymbol{\nu}') = \Phi(\lambda, \boldsymbol{\nu}) + \Phi(\lambda, \boldsymbol{\nu}') - \Phi(\lambda, \boldsymbol{\nu} + \boldsymbol{\nu}')$,
- differential phase: $\Delta\Phi(\lambda, \boldsymbol{\nu}_m) = \Phi(\lambda, \boldsymbol{\nu}_m) - \Phi(\lambda_{\text{ref}}, \boldsymbol{\nu}_m)$

Due to its technical complexity, very few beam combiners provide a phase reference and rely on these non linear measurements. These non linearities introduce some important difficulties in the image reconstruction task as it worsens the noise statistics and makes the problem non convex (*i.e.* the solution may not be unique and depends on the initialization of the algorithm).

¹ Centre de Recherche Astrophysique de Lyon

2 Image reconstruction

The reconstruction of a monochromatic image from optical interferometry data is a challenging task which has been the subject of fruitful research and resulted in various algorithms. Most of these algorithms can be placed in a *maximum a posteriori* framework: the maximum entropy method BSMEM (Buscher 1994; Baron & Young 2008), WISARD (Meimon et al. 2005), MiRA (Thiébaud 2008), IRBis (Hofmann et al. 2014), PAINTER (Schutz et al. 2014) and MiRA3D which is currently in development at CRAL. As without phase reference the problem is non convex, all these methods that rely on continuous optimization methods may end in some local optima. To provide a better estimate of the global optimum, some authors proposed stochastic methods: MACIM (Ireland et al. 2008) and SQUEEZE (Baron et al. 2010).

Although most beam combiners are now polychromatic only few of these methods (namely: PAINTER, MiRA3D and SQUEEZE) were specifically designed for such hyperspectral data. When dealing with multi-spectral data, a first possibility is to process each wavelength independently and reconstruct a monochromatic image for each subset of measurements from a given spectral channel. For instance, this is what have been done by le Bouquin et al. (2009) for the multi-spectral images of the Mira star T Lep. Another possibility is to exploit some assumed spectral continuity of $I(\lambda, \theta)$ and process the multi-spectral data globally to reconstruct an approximation of the 3-D distribution $I(\lambda, \theta)$. Although demonstrated in a different context of integral field spectral spectroscopy, this latter approach has proven to be more powerful (Soulez et al. 2011; Bongard et al. 2011).

In the continuation of our previous works (Thiébaud & Soulez 2012; Soulez & Thiébaud 2013), this paper briefly describes the MiRA-3D algorithm that exploits the advantages of a global multi-spectral processing of optical interferometric data.

3 The MiRA3D algorithm

In the *maximum a posteriori* framework, the reconstructed image \mathbf{x} is the solution the most probable according to some priors that fit the measurements \mathbf{m} . In other words, it is the best compromise between some priors on the observed object and the fidelity to the data. In MiRA3D, it is achieved by minimizing the sum of a regularization function f_{prior} and a likelihood function (*e.g.* the χ^2 for Gaussian errors). A “so-called” hyperparameter μ is necessary to adjust the compromise between the priors and the agreements to the measurements:

$$\mathbf{x}^+ = \arg \min_{\mathbf{x} \in \mathbb{X}} \mu \underbrace{f_{\text{prior}}(\mathbf{x})}_{\text{regularization}} + \underbrace{f_{\text{data}}(\mathbf{x}|\mathbf{m})}_{\text{likelihood}} \quad (3.1)$$

where \mathbb{X} is the feasible set described by some strict physical based constraints: positivity and normalization:

$$\mathbb{X} = \{\mathbf{x} \in \mathbb{R}^n : \mathbf{x} \geq 0 ; \forall \lambda, \sum_k x_{k,\lambda} = 1.\} \quad (3.2)$$

Unfortunately, in interferometry the non-linearity of the likelihood function and the constraints on the image make the direct minimization of Eq. (3.1) numerically cumbersome for classical optimization algorithm. To damper this problem, in MiRA 3D, we introduce two auxiliary variables \mathbf{y} and \mathbf{z} and solve:

$$\mathbf{x}^+ = \arg \min_{\mathbf{x}} \mu f_{\text{prior}}(\mathbf{z}) + f_{\text{data}}(\mathbf{y}|\mathbf{m}) \quad \text{s.t.} \quad \begin{cases} \mathbf{y} & = \mathbf{H} \cdot \mathbf{x}, \\ \mathbf{A} \cdot \mathbf{x} & = \mathbf{z}, \\ \mathbf{z} & \geq 0, \\ \sum_{\lambda} \mathbf{x} & = 1. \end{cases} \quad (3.3)$$

where \mathbf{y} is the vector of complex amplitudes involved in each measurement. It is linked to the image \mathbf{x} by the non uniform Fourier operator \mathbf{H} . Depending on the priors \mathbf{z} lies in the image domain (*i.e.* $\mathbf{A} = \mathbf{Id}$) or any other space linearly mapped by \mathbf{A} . For example, in the case of a classical quadratic smoothing priors acting on spatial gradient, \mathbf{A} is a spatial derivative operator and $f_{\text{prior}}(\mathbf{z}) = \|\mathbf{z}\|^2$. Written this way, the image reconstruction problem is split in 3 much simple problems that are alternatively solved using an Alternating Directing Method of Multiplier (ADMM) (Boyd et al. 2010).

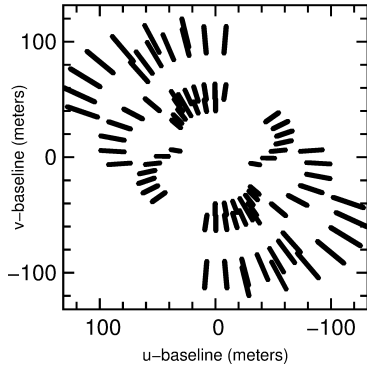
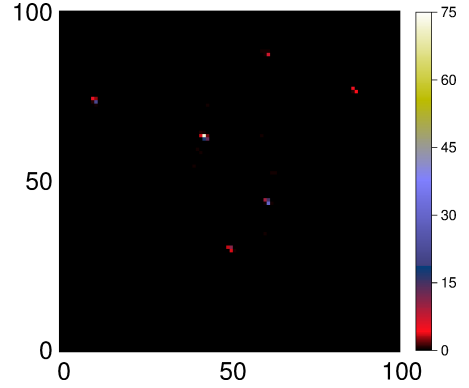
Fig. 1. (u, v) coverage

Fig. 2. Reconstructed image (spectrally integrated)

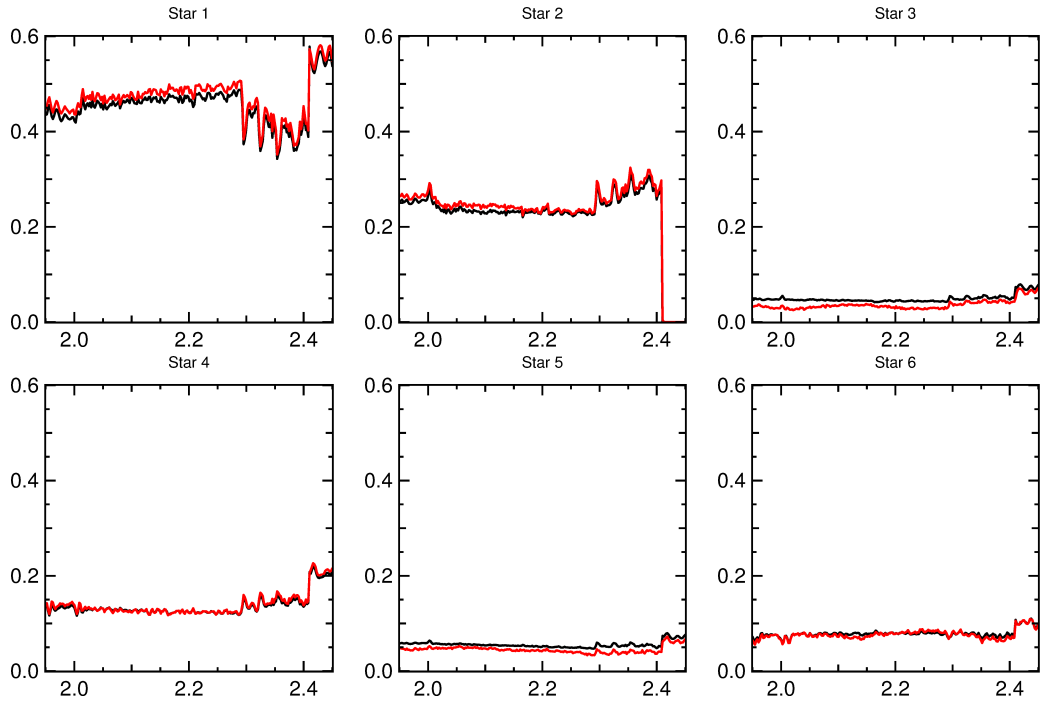


Fig. 3. Estimated (in black) and theoretical (in red) spectra for each 6 stars.

4 Results

4.1 The phase referenced case: GRAVITY

We have tested our method on a simulation of the VLT/ GRAVITY instrument. In its phase referenced mode, it produces multispectral complex visibilities. These complex visibilities depend linearly of the intensity distribution, the reconstruction problem is then convex. The simulated data consists on six unresolved stars with different spectra observed by the 4 UTs with 240 spectral channels from $1.95 \mu\text{m}$ to $2.45 \mu\text{m}$ and 42 baselines (about 10080 complex visibilities). (u, v) coverage is presented Fig. 1.

We reconstruct an hyperspectral image with 240 spectral channels and 100×100 pixels of size 1×1 mas. The prior used is the joint (Fornasier & Rauhut 2008) sparsity that assumes that there are few sources and those sources are located at the same position. The reconstructed image spectrally integrated in the K band is shown Fig. 2. The six stars are recovered and there is not any false detection. The shape of each reconstructed star is due to the beam and its centroid indicated its position with an error lower than 0.15 mas. The 6 reconstructed spectra presented in Fig. 3 are very close to the theoretical spectra.

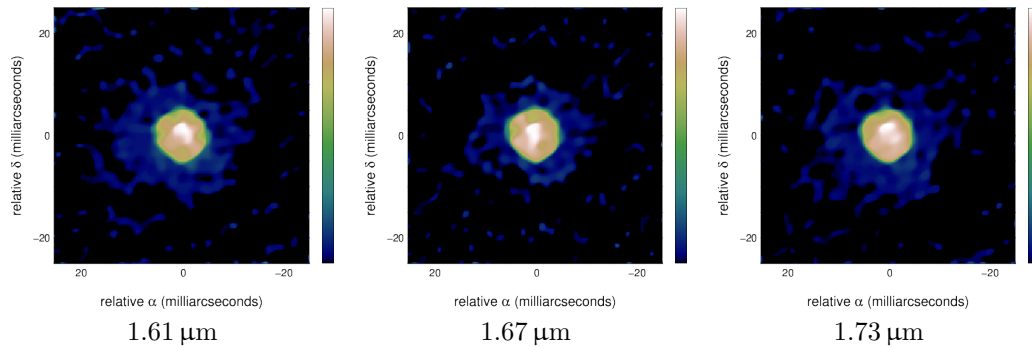


Fig. 4. Reconstruction of the Mira star R Car for the three wavelengths of PIONIER

4.2 Without phase reference: PIONIER

In the context of the “2014 interferometric imaging beauty contest” (Monnier et al. 2014), we have reconstructed image of the oxygen rich Mira R Car. This data was acquired using PIONIER in the context of a technical run aiming at demonstrating VLTI imaging capability. PIONIER is the first four beams combiner of the VLTI. It provides powerspectra and closure phase in 3 spectral channels in H band. Contrary to the GRAVITY phase referenced case, the reconstruction problem is non convex. It is regularized using the multi-spectral total variation (Sapiro & Ringach 1996). This prior favors smooth objects while preserving sharp edges and favors colocalization of those edges along spectral dimension.

In the reconstructed image presented Fig. 4, the R Car object is composed of a disk of about 10 mas in diameter. This disk is not uniform and especially there is marginally resolved brighter spot (14 % brighter) of about 3 mas in width located 1 mas north of the center of the disk. This disk is surrounded by an approximately circular shell of about 22 mas in diameter. The optical thickness of this shell differs from one spectral channel to another, especially it seems to be more optically thin in the 1.67 μm than in the 1.61 μm .

The author thanks T. Paumard who provides the GRAVITY simulated data and J.P. Berger who provides the R Car data.

Our algorithm has been implemented and tested with YORICK (<http://yorick.sourceforge.net/>) which is freely available.

This work is supported by the POLCA project (*Percées astrophysiques grâce au traitement de données interférométriques polychromatiques* funded by the French ANR: ANR-10-BLAN-0511).

References

- Baron, F., Monnier, J. D., & Kloppenborg, B. 2010, in SPIE Astronomical Telescopes+ Instrumentation, International Society for Optics and Photonics, 77342I–77342I
- Baron, F. & Young, J. S. 2008, in SPIE Conference, Vol. 7013, 144
- Bongard, S., Soulez, F., Thibaut, ., & Pcontal, E. 2011, Monthly Notices of the Royal Astronomical Society, 418, 258
- Boyd, S., Parikh, N., Chu, E., Peleato, B., & Eckstein, J. 2010, Foundations and Trends in Machine Learning, 3, 1
- Buscher, D. F. 1994, in IAU Symp. 158, ed. J. G. Robertson & W. J. Tango, 91–+
- Fornasier, M. & Rauhut, H. 2008, SIAM Journal on Numerical Analysis, 46, 577
- Hofmann, K., Weigelt, G., & Schertl, D. 2014, Astronomy & Astrophysics, 565, A48
- Ireland, M. J., Monnier, J. D., & Thureau, N. 2008, in Proc. SPIE, Vol. 6268, 62681T
- le Bouquin, J.-B., Lacour, S., Renard, S., Thibaut, ., & Merand, A. 2009, Astron. Astrophys., 496, L1
- Meimon, S., Mugnier, L. M., & le Besnerais, G. 2005, Optics Letters, 30, 1809
- Monnier, J. D., Berger, J.-P., Le Bouquin, J.-B., et al. 2014, in SPIE Astronomical Telescopes+ Instrumentation, 91461Q–91461Q
- Sapiro, G. & Ringach, D. L. 1996, IEEE Trans. Image Process., 5, 1582
- Schutz, A., Ferrari, A., Mary, D., et al. 2014, JOSA A, 31, 2334
- Soulez, F. & Thiébaud, E. 2013, in Improving the performances of current optical interferometers, International Colloquium at haute provence observatory, St Michel l’observatoire, France, .
- Soulez, F., Thibaut, ., Bongard, S., & Bacon, R. 2011, in 3rd IEEE WHISPERS, Lisbon, Portugal
- Thiébaud, E. 2008, in Proc. SPIE, Vol. 7013, 70131I
- Thiébaud, É. & Soulez, F. 2012, in SPIE Astronomical Telescopes+ Instrumentation, 84451C–84451C